ISME

# Effects of Temperature on Radiative Properties of Nanoscale Multilayer with Coherent Formulation in Visible Wavelengths

**S.A.A. Oloomi***
Assistant Professor

**A. Saboonchi**†
Associate Professor

**A. Sedaghat**‡
Assistant Professor

*During the past two decades, there have been tremendous developments in near-field imaging and local probing techniques. Examples are the Scanning Tunneling Microscope (STM), Atomic Force Microscope (AFM), Near-field Scanning Optical Microscope (NSOM), Photon Scanning Tunneling Microscope (PSTM), and Scanning Thermal Microscope (SThM).Results showed that the average reflectance for a dopant concentration of* $10^{18} cm^{-3}$ *is 0.28247 in 25ºC, 0.30064 in 500ºC and 0.32052 in 1000ºC for donors. The average reflectance for a dopant concentration of* $10^{18}\,\mathrm{cm}^{-3}$ *is 0.282474 in 25ºC, 0.30064 in 500ºC and 0.32052 in 1000ºC for acceptors. For visible wavelengths, more reflectance occurs in greater temperature and the emittance decreases as the temperature increases. In these wavelengths, transmittance is negligible. At room temperature for concentration less than* $10^{19} cm^{-3}$*, concentration has not important influence on radiative properties. At room temperature, the scattering process is dominated by lattice scattering for lightly doped silicon, and the impurity scattering becomes important for heavily doped silicon when the dopant concentration exceeds* $10^{18} cm^{-3}$.

Archive of SID

*Keyword:* Temperature, Radiative Properties, Nanoscale, Multilayer, Coherent Formulation, Visible Wavelengths

## 1 Introduction

Silicon is semiconductor that plays a vital role in integrated circuits and MEMS/NEMS [1]. Semitransparent crystalline silicon solar cells can improve the efficiency of solar power generation [2]. Accurate radiometric temperature measurements of silicon wafers and heat transfer analysis of rapid thermal processing furnaces require a thorough understanding of the radiative properties of the silicon wafer, whose surface may be coated with dielectric or absorbing films [1]. In fact, surface modification by coatings can significantly affect the radiative properties of a material [3].

* Corresponding Author, Assistant Professor , Department of Mechanical Engineering, Islamic Azad University, Yazd Branch, Yazd, AmirOloomi@iauyazd.ac.ir

† Associate Professor, Department of Mechanical Engineering, Isfahan University of Technology, AhmadSab@cc.iut.ac.ir.

‡ Assistant Professor, Department of Mechanical Engineering, Isfahan University of Technology, Sedaghat@cc.iut.ac.ir

www.SID.ir

Oloomi et al. showed for lightly doped silicon that silicon dioxide and silicon nitride coating act as anti reflector and these coatings reduce reflectance toward bare silicon. If thickness of non metal coating increases, reflectance of multilayer decreases and transmittance increases [4].
This work uses transfer-matrix method for calculating the radiative properties. The coherent formulation is applied. The Drude Model for the Optical Constants of Doped Silicon is employed. In this work, phosphorus and boron are default impurities for n-type and p-type, respectively.

## 2 Modeling

### *2.1 Coherent Formulation*

When the thickness of each layer is comparable or less than the wavelength of electromagnetic waves, the wave interference effects inside each layer become important to correctly predict the radiative properties of multilayer structure of thin films. The transfer-matrix method provides a convenient way to calculate the radiative properties of multilayer structures of thin films (Figure 1).
By assuming that the electromagnetic field in the $j_{th}$ medium is a summation of forward and backward waves in the $z$-direction, the electric field in each layer can be expressed by

$$E_j = \begin{cases} \left[A_1 e^{iq_{1z}z} + B_1 e^{-iq_{1z}z}\right] e^{(iq_x x - i\omega t)}, \; j = 1 \\ \left[A_j e^{iq_{jz}(z - z_{j-1})} + B_j e^{-iq_{jz}(z - z_{j-1})}\right] e^{(iq_x x - i\omega t)}, \; j = 2,3,...N \end{cases} \tag{1}$$

Where $A_j$ and $B_j$ are the amplitudes of forward and backward waves in the $j_{th}$ layer. Detailed descriptions for calculation of $A_j$ and $B_j$ is given in Ref [5].

### *2.2 The Drude Model for the Optical Constants of Doped Silicon*

The complex dielectric function is related to the refractive index (n) and the extinction coefficient ($k$) by this equation

$$\varepsilon(\omega) = (n + ik)^2 \tag{2}$$

To account for the doping effects, the Drude model is employed, and the dielectric function of both intrinsic and doped silicon is expressed as the following form [6]

$$\varepsilon(\omega) = \varepsilon_{bl} - \frac{N_e e^2 / \varepsilon_0 m_e^*}{\omega^2 + i\omega/\tau_e} - \frac{N_h e^2 / \varepsilon_0 m_h^*}{\omega^2 + i\omega/\tau_h} \tag{3}$$

Where the first term in the right ($\varepsilon_{bl}$) accounts for contributions by transitions across the band gap and lattice vibrations, the second term is the Drude term for transitions in the conduction band (free electrons), and the last term is the Drude term for transitions in the valence band (free holes). Here, $N_e$ and $N_h$ are the concentrations, $m_e^*$ and $m_h^*$ the effective masses, $\tau_e$ and $\tau_h$ the scattering times for free electrons and holes, respectively, and e is the electron charge. For simplicity, the effective masses are assumed to be independent of the frequency, dopant concentration, and temperature in the present study, and their values are taken from Ref [7] as:

$$m_e^* = 0.27 m_0 \tag{4}$$

$$m_h^* = 0.37 m_0 \tag{5}$$

Archive of SID

www.SID.ir

where $m_0$ is the electron mass in vacuum. Since $\varepsilon_{bl}$ accounts for all contributions other than the free carriers, it can be determined from the refractive index and extinction coefficient of silicon as [1]:

$$\varepsilon_{bl} = (n_{bl} + ik_{bl})^2 \tag{6}$$

In this work, the expression of Jellison and Modine [8] is used to calculate the refractive index $n_{bl}$ in the wavelength region from 0.5 μm to 0.84 μm.

$$n_{bl}(\lambda, T) = n_0(\lambda) + \beta(\lambda)T \tag{7}$$

$$n_0 = \sqrt{4.565 + \frac{97.3}{3.648^2 - (1.24/\lambda)^2}} \tag{8}$$

$$\beta(\lambda) = -1.864\times 10^{-4} + \frac{5.394\times 10^{-3}}{3.648^2 - (1.24/\lambda)^2} \tag{9}$$

The extinction coefficient $k_{bl}$ accounts for the band gap absorption as well as the lattice absorption. The band gap absorption occurs when the photon energy is greater than the band gap energy of silicon and results in a large absorption coefficient. The absorption coefficient is related to the extinction coefficient as:

$$\alpha = 4\pi k/\lambda \tag{10}$$

$k_{bl}$ can be determined for all temperatures from the equation for absorption coefficients. In the present study, the extinction coefficient of silicon is calculated from Jellison and Modine's expression in the wavelength range from 0.4 to 0.9 μm as follows [8]:

$$k_{bl}(\lambda, T) = k_0(\lambda)\exp\left[\frac{T}{369.9 - \exp(-12.92 + 6.831/\lambda)}\right] \tag{11}$$

$$k_0(\lambda) = -0.0805 + \exp\left[-3.1893 + \frac{7.946}{3.648^2 - (1.24/\lambda)^2}\right] \tag{12}$$

The scattering time $\tau_e$ or $\tau_h$ depends on the collisions of electrons or holes with lattice (phonons) and ionized dopant sites (impurities or defects); hence, it generally depends on the temperature and dopant concentration. The total scattering time (for the case of $\tau_e$), which consists of the above two mechanisms, can be expressed as [9]:

$$\frac{1}{\tau_e} = \frac{1}{\tau_{e-l}} + \frac{1}{\tau_{e-d}} \tag{13}$$

Where $\tau_{e-l}$ and $\tau_{e-d}$ denote the electron-lattice and electron-defect scattering time, respectively. Similarly, $\tau_h$ can be related to $\tau_{h-l}$ and $\tau_{h-d}$ . In addition, the scattering time τ is also related to the mobility μ by:

$$\tau = m^*\mu/e \tag{14}$$

At room temperature, the total scattering time $\tau_e^0$ or $\tau_h^0$ , which depends on the dopant concentration, can be determined from the fitted mobility equations [10]:

$$\mu_e^0 = \frac{1268}{1 + (N_D/1.3\times 10^{17})^{0.91}} + 92 \tag{15}$$

Archive of SID

www.SID.ir

$$\mu_h^0 = \frac{447.3}{1 + (N_A / 1.9 \times 10^{17})^{0.76}} + 47.7 \tag{16}$$

where superscript 0 indicates values at 300 K and $N_D$ or $N_A$ is the dopant concentration of donor (phosphorus, n-type) or acceptor (boron, p-type) in $cm^{-3}$. Consequently, the scattering time from impurity contribution $\tau_{e-d}^0$ or $\tau_{h-d}^0$ can be determined from Equation. (13) by knowing the total scattering time and that due to lattice contribution. Because of the relatively insignificance of impurity scattering at high temperatures, the following formula can be used to calculate the impurity scattering times:

$$\frac{\tau_{e-d}}{\tau_{e-d}^0} = \frac{\tau_{h-d}}{\tau_{h-d}^0} = \left(\frac{T}{300}\right)^{1.5} \tag{17}$$

In order to obtain a better agreement with the measured near-infrared absorption coefficients for lightly doped silicon [1, 11], the expressions for lattice scattering are modified in the present study, as follows:

$$\tau_{e-l} = \tau_{e-l}^0 (T/300)^{-3.8} \tag{18}$$

$$\tau_{h-l} = \tau_{h-l}^0 (T/300)^{-3.6} \tag{19}$$

## 3 Results

Consider the case in which the silicon wafer is coated with a silicon dioxide layer on both sides. The thickness of silicon wafer is 500 $\mu m$ and the Electromagnetic waves are incident at $\theta = 0^\circ$. The considered wavelength range is $0.5\mu m < \lambda < 0.7\mu m$. Doped silicon is used and the coherent formulation is applied. The thickness of $SiO_2$ is 400 nm. The Drude Model for the Optical Constants of Doped Silicon is employed. The optical constants of silicon dioxide and silicon nitride are mainly based on the data collected in Palik's handbook [12]. Phosphorus acts as donor (n-type) and born acts as acceptor (p-type) for doped silicon. Impurities concentration differs from $10^{17} cm^{-3}$ to $10^{19} cm^{-3}$ for both of donors and acceptors. Different temperatures are applied for the case showed above. Some results of this study are shown below in figures 2 to 5 and tables 1 to 2.

## 4 Conclusions

The effect of wave interference can be understood by plotting the spectral properties such as reflectance or transmittance of a thin dielectric film versus the film thickness and analyzing the oscillations of properties due to constructive and destructive interferences [13-14]. The fluctuations in the results are observed because of the wave's interferences, these fluctuations are in the shape of sinus curves and with increasing wavelength, the distance between peaks grows [13].

Results showed that the average reflectance for a dopant concentration of $10^{18} cm^{-3}$ is 0.28247 in 25ºC, 0.30064 in 500ºC and 0.32052 in 1000ºC for donors. The average reflectance for a dopant concentration of $10^{19} cm^{-3}$ is 0.282474 in 25ºC, 0.30064 in 500ºC and

Archive of SID

www.SID.ir

0.32052 in 1000ºC for acceptors (Table 1). It may be concluded that average reflectance decreases with increasing concentration.

For visible wavelengths, more reflectance occurs in greater temperature (Figures 2 and 5) and the emittance decreases as the temperature increases (Figure 4). In these wavelengths, transmittance is negligible (Figure 3).

It was also observed that the average emittance for a dopant concentration of $10^{18} cm^{-3}$ is 0.71753 in 25ºC, 0.699356 in 500ºC and 0.679478 in 1000 ºC for donors. This is while the average emittance value for a dopant concentration of $10^{18} cm^{-3}$ is 0.717526 in 25ºC, 0.699352 in 500 ºC and 0.679474 in 1000ºC for acceptors (Table 2). Donor impurities and acceptor impurities act similar in visible wavelengths but donor impurities have greater emittance than acceptor impurities.

At room temperature for concentration less than $10^{19}\,\mathrm{cm}^{-3}$, concentration has not important influence on radiative properties. At room temperature, the scattering process is dominated by lattice scattering for lightly doped silicon, and the impurity scattering becomes important for heavily doped silicon when the dopant concentration exceeds $10^{18}\,\mathrm{cm}^{-3}$.

## References

[1] Timans, P.J., "*The Thermal Radiative Properties of Semiconductors*" Advances in Rapid Thermal and Integrated Processing, Academic Publishers, Dordrecht, Netherlands, pp. 35-102, (1996).

[2] Fath, P., Nussbaumer, H., and Burkhardt, R., "Industrial Manufacturing of Semitransparent Crystalline Silicon Power Solar Cells", Sol. Energy Mater. Sol. Cells; Vol. 74, pp. 127–131, (2002).

[3] Makino, T., "Thermal Radiation Spectroscopy for Heat Transfer Science and for Engineering Surface Diagnosis", Int. Journal, Heat Transfer, Vol. 1, pp. 55–66, (2002).

[4] Oloomi, S.A.A, Saboonchi, A., and Sedaghat, A., "Effects of Thin Film Thickness on Emittance, Reflectance and Transmittance of Nano Scale Multilayers ", International Journal of the Physical Sciences, Vol. 5, No. 5, pp. 465-469, (2010).

[5] Fu, C.J., Zhang, Z.M., and Zhu, Q.Z., "Optical and Thermal Radiative Properties of Semiconductors Related to Micro/Nanotechnology," Advances in Heat Transfer, Vol. 37, pp. 179-296, (2003).

[6] Hebb, J. P., "Pattern Effects in Rapid Thermal Processing," Ph.D Thesis, Department of Mechanical Engineering, Massachusetts Institute of Technology, Cambridge, MA, (1997).

[7] Spitzer, W. G., and Fan, H. Y., "Determination of Optical Constants and Carrier Effective Mass of Semiconductors," Phys. Rev., Vol. 1, pp. 882-890, (1957).

[8] Jellison, G. E., and Modine, F. A., "Optical Functions of Silicon at Elevated Temperatures," J. Appl. Phys., Vol .76, pp. 3758-3761, (1994).

[9] Sze, S. M., *Semiconductor Devices, Physics and Technology*, 2nd ed, Wiley, New York (2002).

Archive of SID

www.SID.ir

[10] Beadle, W. E., Tsai, J. C. C., and Plummer, R. D., "*Quick Reference Manual for Silicon Integrated Circuit Technology*", Wiley, New York, (1985).

[11] Rogne, H., Timans, P. J., and Ahmed, H., "Infrared Absorption in Silicon at Elevated Temperatures", Appl. Phys. Lett., Vol. 69, pp. 2190-2192, (1996).

[12] Palik, E.D, "Silicon Dioxide ($SiO_2$)," and "Silicon Nitride ($Si_3N_4$)," *Handbook of Optical Constants of Solids*, San Diego, CA, (1998).

[13] Oloomi, S.A.A, Saboonchi, A., and Sedaghat, A., "Parametric Study of Nanoscale Radiative Properties of Doped Silicon Multilayer Structures", World Applied Sciences Journal, Vol. 8, No 10, pp. 1200-1204, (2010).

[14] Oloomi, S.A.A, Saboonchi, A., and Sedaghat, A., "Effects of Thin Films' Thickness on Radiative Properties of Doped Silicon Multilayer Structures", Middle-East Journal of Scientific Research , Vol. 5, No 4, pp. 210-213, (2010).

## Nomenclature

$A_j$ : Amplitude of forward waves in the $j_{th}$ layer
$B_j$ : Amplitude of backward waves in the $j_{th}$ layer
$k$ : Extinction coefficient
$m_0$ : Electron mass in vacuum
$m_e^*$ : Effective masses for free electrons
$m_h^*$ : Effective masses for free holes
$n$ : Refractive index

$N_e$ : Concentrations for free electrons
$N_h$ : Concentrations for free holes

*Greek symbols*
$\alpha$ : Absorption coefficient
$\mu$ : Mobility
$\tau_e$ : Scattering times for free electrons
$\tau_h$ : Scattering times for holes

Archive of SID

www.SID.ir

## Figures

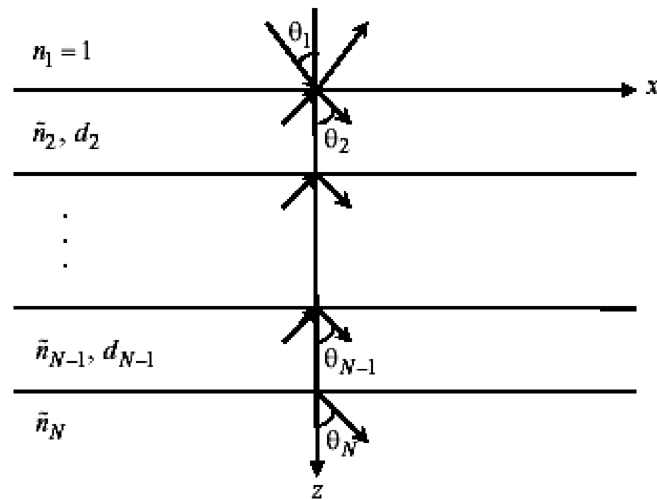


**Figure 1** The geometry for calculating the radiative properties of a multilayer structure

SID

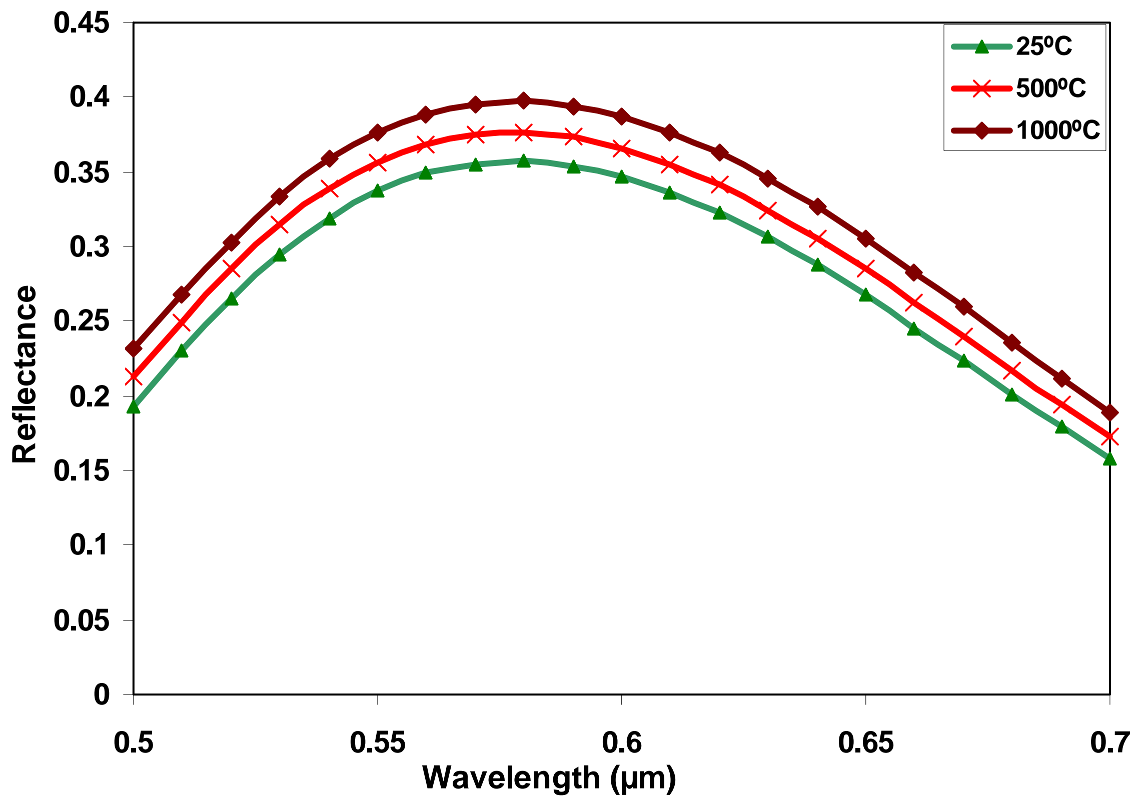


**Figure 2** Spectral Reflectance of silicon wafer coated by silicon dioxide film on both sides with doped silicon (n-type) with $10^{18}\,cm^{-3}$ concentrations, at room Temperatures and normal incidence for visible wavelengths

www.SID.ir

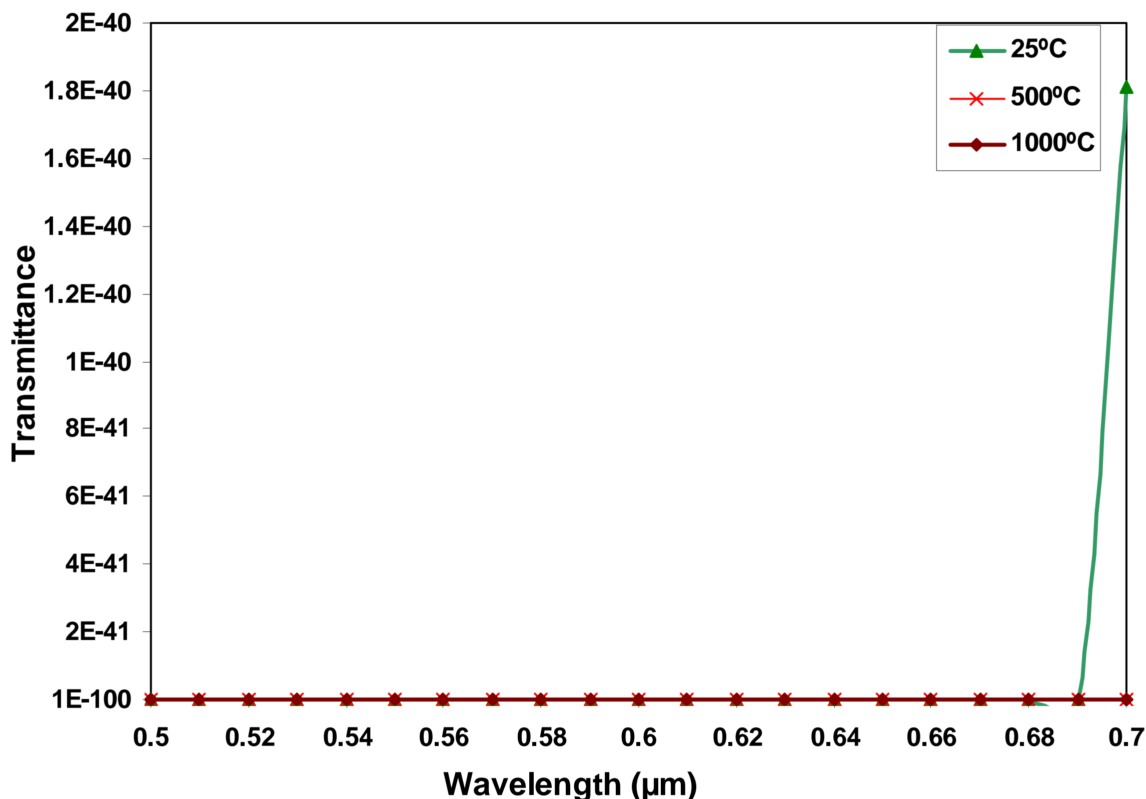


**Figure 3** Spectral Transmittance of silicon wafer coated by silicon dioxide film on both sides with doped silicon (p-type) with $10^{18}\,cm^{-3}$ concentrations, at room Temperatures and normal incidence for visible wavelengths

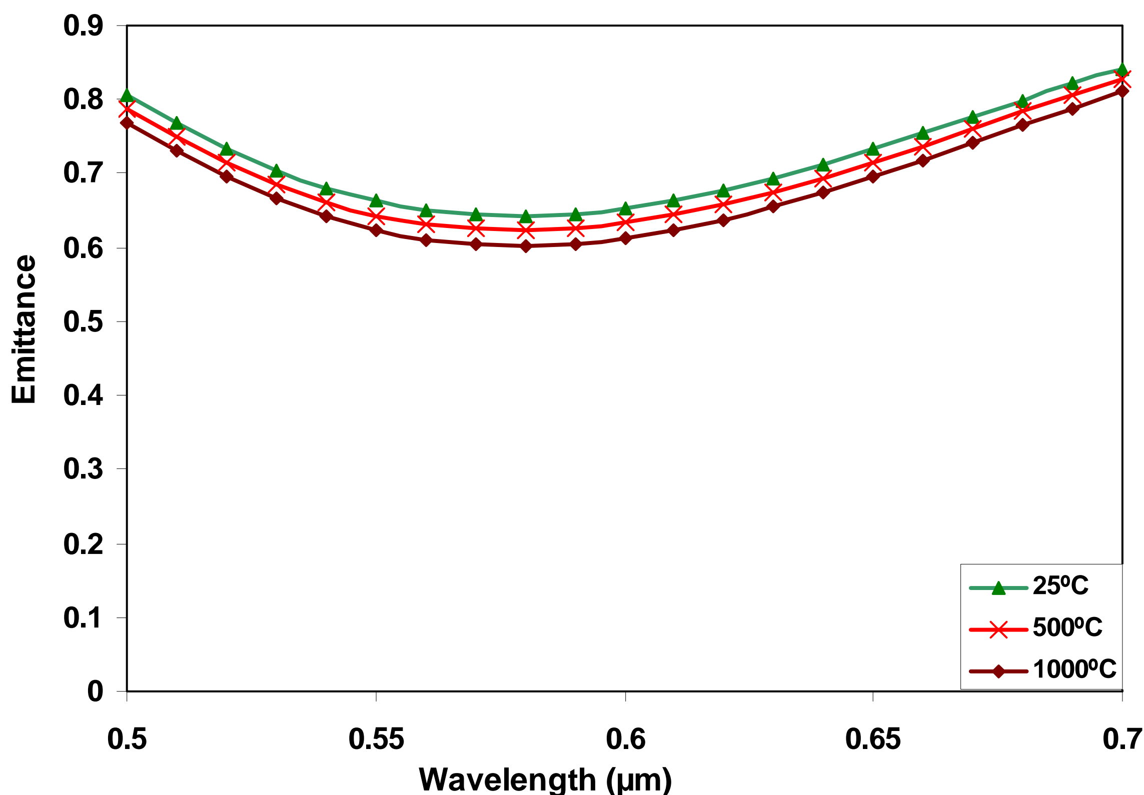


**Figure 4** Spectral Emittance of silicon wafer coated by silicon dioxide film on both sides with doped silicon (n-type) with $10^{17}\,cm^{-3}$ concentrations, at room Temperatures and normal incidence for visible wavelengths

www.SID.ir

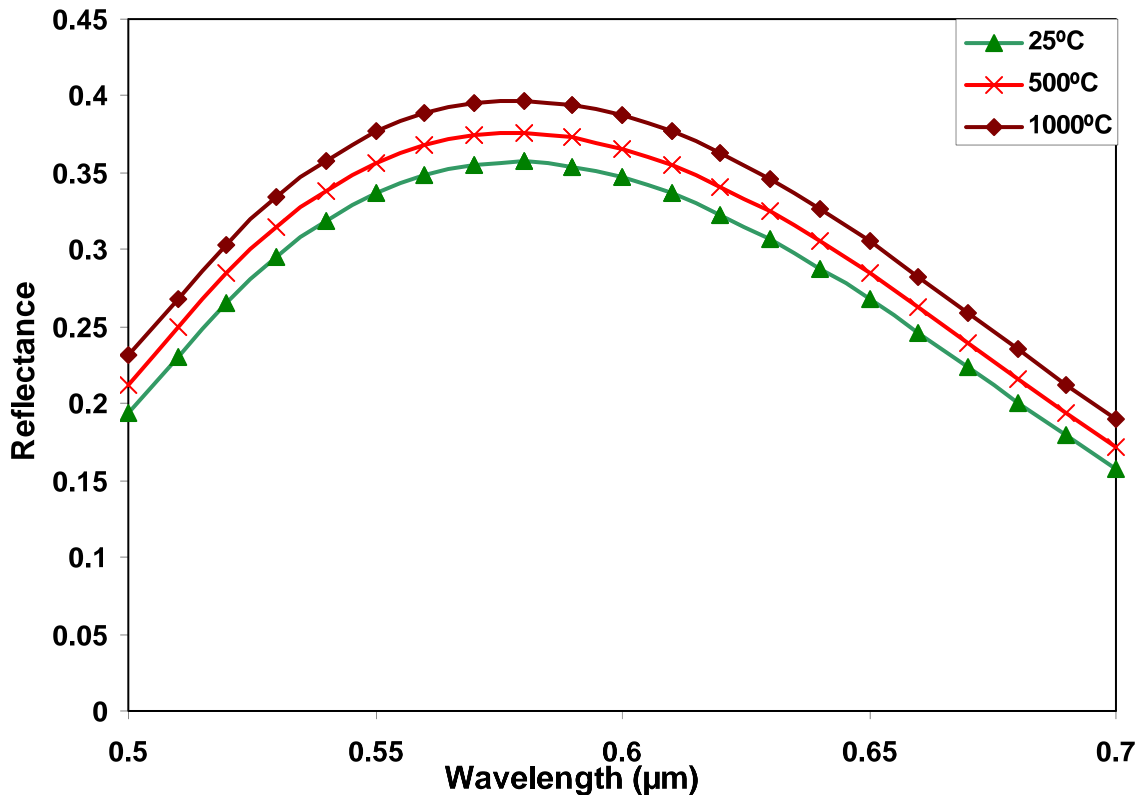


**Figure 5** Spectral Reflectance of silicon wafer coated by silicon dioxide film on both sides with doped silicon (p-type) with $10^{19}\,cm^{-3}$ concentrations, at room Temperatures and normal incidence for visible wavelengths

Archive of

## Tables

**Table 1** Average Reflectance in Visible wavelengths for different impurities and temperatures

| **Temperature/Impurity** | Donors $10^{17}\,cm^{-3}$ | Donors $10^{18}\,cm^{-3}$ | Donors $10^{19}\,cm^{-3}$ | Acceptors $10^{18}\,cm^{-3}$ |
|---|---|---|---|---|
| 25ºC | 0.28248 | 0.2824701 | 0.282426 | 0.282474 |
| 500ºC | 0.300654 | 0.3006438 | 0.300555 | 0.300648 |
| 1000ºC | 0.320524 | 0.3205224 | 0.320491 | 0.320526 |

**Table 2** Average Emittance in Visible wavelengths for different impurities and temperatures

| **Temperature/Impurity** | Donors $10^{17}\,cm^{-3}$ | Donors $10^{18}\,cm^{-3}$ | Donors $10^{19}\,cm^{-3}$ | Acceptors $10^{18}\,cm^{-3}$ |
|---|---|---|---|---|
| 25ºC | 0.71752 | 0.71753 | 0.717574 | 0.717526 |
| 500ºC | 0.699346 | 0.699356 | 0.699445 | 0.699352 |
| 1000ºC | 0.679476 | 0.679478 | 0.679509 | 0.679474 |

www.SID.ir

## چکیده

طی دو دهه اخیر توسعه زیادی در روشهای عکس برداری نزدیک و پیمایشگرهای محلی رخ داده است. به عنوان مثال می توان به میکروسکوپ تونل زنی پویشی (STM) , میکروسکپ نیروی اتمی (AFM) , میکروسکپ نوری پویشگر نزدیک (NSOM) , میکروسکپ تونل زنی پویشی فوتونی (PSTM) و میکروسکپ پویشی حرارتی(SThM) اشاره نمود.

نتایج نشان دادند که بازتاب میانگین برای یونهای دهنده با غلظت $10^{18}$ $cm^{-3}$ برابر است با ۰/۲۸۲۴۷ در دمای ۲۵ºC, ۰/۳۰۰۶۴ در دمای ۵۰۰ºC و ۰/۳۲۰۵۲ در دمای ۱۰۰۰ºC , و بازتاب میانگین برای یونهای پذیرنده با غلظت $10^{18}$ $cm^{-3}$ برابر است با ۰/۲۸۲۴۷ در دمای ۲۵ºC , ۰/۳۰۰۶۴۸ در دمای ۵۰۰ºC و ۰/۳۲۰۵۲۶ در دمای ۱۰۰۰ºC. در طول موج مرئی بازتاب بیشتر در دماهای بالاتر رخ می دهد و ضریب صدور با افزایش دما کاهش میابد. در این طول موجها ضریب عبور قابل صرفنظر کردن است. در دمای اتاق برای غلظت ناخالصی کمتر از $10^{19}$ $cm^{-3}$, غلظت اثر مهمی بر خواص تشعشعی ندارد. در دمای اتاق پدیده پراکندگی توسط تفرق شبکه حائز اهمیت است و پدیده تفرق توسط ناخالصی ها هنگامی موثر واقع می گردد که غلظت ناخالصی به $10^{18}$ $cm^{-3}$ برسد.


Archive of SID

www.SID.ir